

“Scars” in parametrically excited surface waves

Oded Agam^a and Boris L. Altshuler^b

^a *The Racah Institute of Physics, The Hebrew University, Jerusalem 91904, Israel.*

^b *Physics Department, Princeton University, Princeton, NJ 08544
and NEC Research Institute, 4 Independence Way, Princeton, NJ 08540.*

We consider the Faraday surface waves of a fluid in a container with a non-integrable boundary shape. We show that, at sufficiently low frequencies, the wave patterns are “scars” selected by the instability of the corresponding periodic orbits, the dissipation at the container side walls, and interaction effects which reflect the nonlinear nature of the Faraday waves. The results explain the observation of a limited number of scars with anomalous strengths in recent experiments by Kudrolli, Abraham and Gollub.

A prominent feature of wave chaos is the “scar” phenomenon¹. Namely, wave functions are concentrated along the short periodic orbits of the underlying classical system. In general, the phenomenon appears whenever the Eikonal approximation holds, and the corresponding rays exhibit ballistic chaotic dynamics. Since their discovery by numerical studies¹, scars have been observed experimentally in microwave cavities², tunneling diodes³, and capillary waves⁴.

However, theoretical studies of scars⁵ have not addressed several factors which may be present in real systems, such as dissipation, external forcing, nonequilibrium effects, and interactions associated with nonlinear terms of the wave equations. In this Letter we study a system where these factors are significant: the surface waves⁶ in a container of non-integrable shape.

This work was motivated by recent experiments of Kudrolli et al. who studied Faraday waves in a stadium shaped container⁷. The surface waves were excited parametrically by oscillating the container in direction perpendicular to the fluid surface at rest. The experimental findings are quite intriguing, see Fig. 1: I. Out of all known scars of the stadium billiard¹ only three scarring patterns were identified; II. These patterns appear in, approximately, 90% of the cases, and their magnitudes, compared to the random background, is unexpectedly large; III. While probability densities associated with eigenstates of the stadium billiard were always symmetric, nonsymmetric wave patterns have been also observed.

The purpose of this Letter is to explain this behavior. In particular, we show that the excitation threshold for observation of a scarring pattern is governed by the Lyapunov exponent of the corresponding periodic orbit, bulk dissipation, and dissipation at the boundary of the vessel. These factors suppress most of the scarring patterns as well as the random background. The amplitudes of those scars which still can be excited are determined by nonlinear effects. These effects (interactions) also break the symmetry between degenerate scars, which results in nonsymmetric wave patterns.

To begin with, consider the surface waves of an infinite system with an infinite fluid depth. Within the linear approximation, the amplitude of a plain wave, $a_{\mathbf{k}}e^{i\mathbf{k}\cdot\mathbf{r}}$,

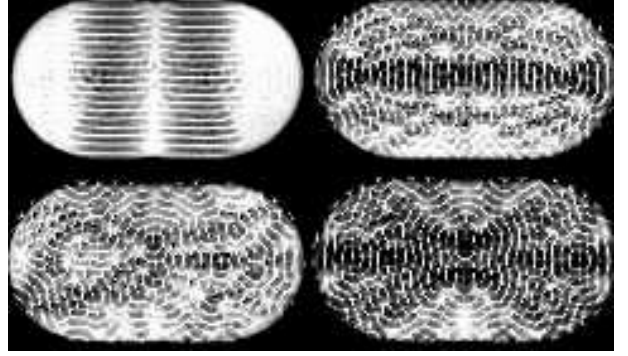


FIG. 1. Surface wave patterns in a stadium shaped container at various external frequencies. Adapted from Ref. 7

satisfies the equation⁶:

$$\frac{\partial^2 a_{\mathbf{k}}}{\partial t^2} + 2\gamma_b \frac{\partial a_{\mathbf{k}}}{\partial t} + \omega_k^2 a_{\mathbf{k}} = 0, \quad (1)$$

where k is the wave number, $\gamma_b = \nu k^2$ is the bulk dissipation rate, and ν is the viscosity. The angular frequency, ω_k , satisfies the dispersion relation:

$$\omega_k^2 = gk + \frac{\Sigma}{\rho} k^3, \quad (2)$$

where g is the acceleration of gravity, Σ is the surface tension, and ρ is the fluid density.

In a finite system, the boundary causes two effects. First, it leads to quantization of the wave vector $k \rightarrow k_\alpha$ (thus also $\omega_k \rightarrow \omega_\alpha$). When the container is rim full, the fluid surface is believed to be pinned to boundary⁸. Thus the eigenmodes of the surface waves, $\psi_\alpha(\mathbf{r})$, are solutions of the Helmholtz equation in a domain of the container shape with Dirichlet boundary conditions.

The second effect of the boundary is an additional dissipation due to the viscous flow in the vicinity of the container side walls. This dissipation, in a system with size L , is of the order $\sqrt{\nu\omega}/L$. For large containers it is negligible compared to the bulk dissipation rate. However, in small systems and for specific wave patterns, this dissipation becomes comparable to γ_b .

Parametric excitation of surface waves, due to vertical shaking, is accounted by introducing time dependent

acceleration, $g \rightarrow g + A \cos(2\omega t)$, into Eq. (1). The parameter space (ω, A) of the resulting Mathieu equation is characterized by tongues of instability where $a_{\mathbf{k}}(t)$ grows exponentially in time. This growth saturates due to nonlinear effects.

To take these interactions into account, it is convenient to employ a formalism analogous to second quantization⁹. For simplicity, we first consider an infinite system. Let us introduce the amplitude variables, $a_{\mathbf{k}}^*$ and $a_{\mathbf{k}}$, analogous to boson creation and annihilation operators at momentum state \mathbf{k} . These variables are c -numbers which can be viewed as boson operators in the limit of a large number of particles. The equations of motion, then, take the form:

$$\frac{\partial}{\partial t} a_{\mathbf{k}} + \gamma_b a_{\mathbf{k}} = -i \frac{\partial \mathcal{H}}{\partial a_{\mathbf{k}}^*}, \quad (3)$$

where \mathcal{H} is the Hamiltonian of the system which consists of three terms: $\mathcal{H} = \mathcal{H}_0 + \mathcal{H}_P + \mathcal{H}_{\text{int}}$. The first component, $\mathcal{H}_0 = \sum_{\mathbf{k}} \omega_k a_{\mathbf{k}}^* a_{\mathbf{k}}$, describes the unforced surface waves in the linear approximation, i.e. Eq. (1).

The second component, \mathcal{H}_P , is the pumping Hamiltonian responsible for the parametric excitation of the Faraday waves. Confining our attention to excitations near the threshold of the first instability tongue of the Mathieu equation, we can write \mathcal{H}_P as

$$\mathcal{H}_P = \frac{1}{2} \sum_k h a_{\mathbf{k}}^* a_{-\mathbf{k}}^* e^{i2\omega t} + C.c.; \quad h = \frac{Ak\omega^2}{4\omega_k}, \quad (4)$$

where A and 2ω are the amplitude and the frequency of the vibrations. In the quadratic approximation, $\mathcal{H} \simeq \mathcal{H}_0 + \mathcal{H}_P$, the equations of motion (3) yield

$$a_{\mathbf{k}}, a_{\mathbf{k}}^* \propto e^{\sigma t}, \quad \text{where } \sigma = -\gamma_b + \sqrt{h^2 - (\omega - \omega_k)^2}. \quad (5)$$

Thus the threshold for instability, at resonance ($\omega = \omega_k$), is $h \geq \gamma_b$. Under this condition, the rate of energy pumped into the system exceeds the dissipation rate.

The third component of the Hamiltonian, \mathcal{H}_{int} , is an interaction term. In the mean field approximation it takes the form⁹

$$\mathcal{H}_{\text{int}} = \sum_{\mathbf{k}\mathbf{k}'} I_k^{(1)}(\theta) |a_{\mathbf{k}}|^2 |a_{\mathbf{k}'}|^2 + I_k^{(2)}(\theta) a_{\mathbf{k}}^* a_{-\mathbf{k}'}^* a_{\mathbf{k}} a_{-\mathbf{k}}, \quad (6)$$

where $I_k^{(j)}(\theta) = T_k^{(j)}(\theta) + i\Gamma_k^{(j)}(\theta)$ are complex matrix elements which depend on the length of the vectors, $k = |\mathbf{k}| = |\mathbf{k}'|$ as well as the angle, θ , between them. The exact form of these matrix elements has been derived by Milner¹⁰. Here we only note that the interaction is local and T is of order ωk^2 , while $\Gamma \propto \nu k^4$.

Several mechanisms limit the exponential growth of the wave amplitude. They are related to different components of the interaction matrix elements. For instance, $\Gamma_k^{(j)}(\theta)$ are associated with nonlinear damping¹⁰, while $T_k^{(2)}(\theta)$ governs the missphasing mechanism¹¹. Missphasing is the phase difference between the pump and the

excited wave, which appears due to the nonlinearity and suppresses the energy absorption.

The actual limiting mechanism is determined by the system size and the excitation frequency. In large systems, boundary effects can be neglected, and patterns are selected by the local properties of the wave equation. This is the regime of pattern formation, where the real parts of the interaction terms merely renormalize h and ω_k . The dominant limiting mechanism, in this case, is nonlinear damping¹⁰. In small systems, contrarily, the wave patterns are globally determined by the boundary, and missphasing turns out to be more effective.

A system can be considered as small provided that the dissipation time, $1/\nu k^2$, exceeds the typical time it takes a surface wave to cross the system. For capillary waves ($k > \sqrt{g\rho/\Sigma}$) this requirement yields the inequality

$$\omega < \omega_c = \frac{\Sigma}{L\rho\nu}. \quad (7)$$

In what follows we assume that this condition is satisfied, the wave patterns are determined by the boundary, and missphasing is the dominant limiting mechanism¹².

Consider now the Faraday waves in a container of non-integrable boundary shape having no discrete symmetries. The modes of the corresponding linear wave equation, $\psi_\alpha(\mathbf{r})$, are eigenstates of a billiard system of the shape of the container. Thus, $\psi_\alpha(\mathbf{r})$ are approximately random Gaussian functions scarred by the periodic orbits of the underlying classical dynamics¹. In principle, one can use $\psi_\alpha(\mathbf{r})$ as a basis for the many body approach described above. However, this basis is inconvenient. In the experiment, several modes are excited simultaneously (approximately 10), and the resulting wave patterns are determined by properties of the short time dynamics of the system. Therefore, it is more natural to use scars as the skeleton of the excited wave patterns.

Below we develop a ‘‘scar representation’’. Instead of dealing with the amplitudes, $n_\alpha = |a_\alpha|^2$, of the eigenfunctions, $\psi_\alpha(\mathbf{r})$, we consider the amplitudes of scars. Using Wigner representation, one can present \mathcal{H}_0 as

$$\mathcal{H}_0 = \sum_\alpha \omega_\alpha n_\alpha = \int \epsilon d\epsilon \int d\mathbf{x} W(\mathbf{x}; \epsilon) n(\mathbf{x}) \quad (8)$$

where $\mathbf{x} = (\mathbf{r}, \mathbf{k})$ is a phase space coordinate, $n(\mathbf{x})$ is the wave amplitude at \mathbf{x} , and $W(\mathbf{x}; \epsilon)$ is the Wigner representation of the imaginary part of the Green function⁵:

$$W(\mathbf{x}; \epsilon) = \sum_\alpha \delta(\epsilon - \omega_\alpha) \int d\mathbf{q} e^{i\mathbf{k}\cdot\mathbf{q}} \psi_\alpha(\mathbf{r} - \frac{\mathbf{q}}{2}) \psi_\alpha^*(\mathbf{r} + \frac{\mathbf{q}}{2}).$$

Assuming the semiclassical limit $kL \gg 1$ as well as the capillary regime, $k > (g\rho/\Sigma)^{1/2}$, we can approximate $W(\mathbf{x}; \epsilon)$ as

$$W(\mathbf{x}; \epsilon) \simeq \delta[\epsilon - H_0(\mathbf{x})] \left(1 + \sum_p W_p(\mathbf{x}; \epsilon) \right), \quad (9)$$

where $H_0(\mathbf{x}) = (\Sigma k^3/\rho)^{1/2}$. The first term in the parenthesis is the average of the random excitation over the energy shell. The second term is a sum over the primitive periodic orbits of the system, p . Each term of this sum represents the corresponding scar contribution:

$$W_p(\mathbf{x}; \epsilon) \simeq 4\pi \text{Re} \frac{e^{-\frac{u_p}{2} + i(S_p - \varphi_p)}}{1 - e^{-\frac{u_p}{2} + i(S_p - \varphi_p)}} \tilde{\delta}(\mathbf{X}_p). \quad (10)$$

Here $S_p(\omega) = l_p(\rho\omega^2/\Sigma)^{1/3}$ is the action of the periodic orbit with length l_p , instability exponent u_p , and Maslov phase φ_p . \mathbf{X}_p denotes a coordinate on the Poincare section of the periodic orbit. The function $\tilde{\delta}(\mathbf{X}_p)$ is localized along the p -th periodic orbit with the width of order $\sqrt{L/k}$. Its integral is unity so that $\tilde{\delta}(\mathbf{X}_p)$ becomes a δ -function in the classical limit⁵ (i.e. at $k \rightarrow \infty$).

Substituting (9) in (8), we obtain

$$\mathcal{H}_0 = \int d\epsilon \epsilon \bar{d}(\epsilon) \bar{n}(\epsilon) + \sum_{p,m} \omega_p^{(m)} n_p, \quad (11)$$

where $\bar{d}(\epsilon) = \mathcal{A}(\rho^2\epsilon/\Sigma^2)^{1/3}/3\pi$ is the mean density of states in a container of area \mathcal{A} ,

$$\bar{n} = \frac{1}{d} \int d\mathbf{x} \delta[\epsilon - H_0(\mathbf{x})] n(\mathbf{x}) \quad (12)$$

is the average amplitude of the random background, and

$$n_p = \frac{1}{t_p} \oint dt n(\mathbf{x}_p(t)) \quad (13)$$

is the amplitude of the scar p . Here t_p is the period of the corresponding orbit, and $\mathbf{x}_p(t)$ is its coordinates parameterized by the time. The eigenfrequencies of the scars, $\omega_p^{(m)}$, are the poles of (10), i.e. the solutions of the equation $S_p(\omega_p^{(m)}) = 2\pi m + \varphi_p - iu_p/2$. Expanding to leading order in u_p we have

$$\omega_p^{(m)} \simeq \left(\frac{2\pi m + \varphi_p}{l_p(\rho/\Sigma)^{1/3}} \right)^{3/2} - i \frac{\lambda_p}{2}, \quad (14)$$

where $\lambda_p = u_p/t_p$ is the Lyapunov exponent of the orbit.

Now one can substitute the Hamiltonian (11) into the equations of motion (3) and see that the Lyapunov exponent plays the role of a dissipation. Indeed, $\lambda_p/2$ is the rate at which the ‘‘particle escapes from the scar’’. This rate should be added to the dissipation rate. The Lyapunov exponents of few short periodic orbits of the stadium billiard are tabulated in Table I. Comparison of these values with the experimental bulk dissipation rate, $\gamma_b \simeq 2 \text{ sec}^{-1}$, shows that their effect is significant.

Next, we consider the dissipation at the side walls of the container¹³. This dissipation has been calculated for particular cases, e.g., the square and the circular containers¹⁴. From these results it is evident that boundary dissipation depends on the particular form of the wave pattern. To obtain the result for a general container

shape, and arbitrary scarring pattern, we first note that boundary dissipation takes place very close to the boundary, at distance of order $l_D = \sqrt{2\nu/\omega} \sim 10^{-2} \text{ cm}$. Viewing the scar as a plain wave scattered from the boundary, each collision point adds its own contribution to the dissipation rate. These contributions can be calculated by traditional methods¹⁴. Assuming pinning of the fluid surface at the boundary, the resulting dissipation rate of a scar can be presented as a sum over the reflection points of the orbit from the boundary:

$$\gamma_p \simeq \frac{(2\nu\omega)^{1/2}}{l_p} \sum_n \frac{1 - \frac{1}{2} \cos^2(\theta_n)}{\cos(\theta_n)}, \quad (15)$$

where θ_n is the angle between the orbit and the normal to the boundary. Examples of γ_p for various scars of the stadium billiard are presented in Table I. Note that the anomalously large dissipation rate of whispering gallery modes (patterns Nos. 8, 9) results from θ_n being close to $\pi/2$, see (15).

The boundary dissipation of the random background, $\bar{\gamma}$, can be obtained from the result for a long ergodic orbit. However, the result diverges since ergodicity implies that θ_n can become arbitrarily close to $\pi/2$. Cutting this divergence by the wave resolution, $\Delta\theta_n \approx 1/kL$, we obtain

$$\bar{\gamma} \simeq \frac{(2\omega\nu)^{1/2}}{L} \ln(kL). \quad (16)$$

No	pattern	l_p	$\lambda_p/2$	γ_p	No	pattern	l_p	$\lambda_p/2$	γ_p
1		12	0	0.35	10		27	3.4	0.42
2		21	3.9	0.2	11		28.3	4.2	0.39
3		23.1	3.8	0.45	12		28.7	5.0	0.39
4		24	4.8	0.4	13		29.2	6.2	0.8
5		24.2	3.9	0.86	14		37.6	2.4	0.38
6		24.8	6.1	0.8	15		38.1	4.1	0.38
7		26	5.9	0.68	16		49.1	2.4	0.36
8		26.4	6.1	2.2	17		49.3	3.5	0.37
9		27	8.3	1.63	18		∞	4.9	3.0

TABLE I. Parameters of some periodic orbits of the stadium billiard, with dimensions of the experimental system: semicircles radius 3 cm, and distance between semicircles 4.5 cm. l_p is the length of the orbit in centimeters, λ_p is the Lyapunov exponent in sec^{-1} , and γ_p is the contribution to the dissipation rate due to the boundary in sec^{-1} . The velocity is set to be similar to the experimental value, 66 cm/sec.

Collecting the various dissipation terms and the contribution of the Lyapunov exponent, the threshold for excitation of scars at resonance ($\omega = \text{Re } \omega_p^{(m)}$) is:

$$h > h_p = \gamma_b + \gamma_p + \lambda_p/2 \quad (17)$$

Therefore, large boundary dissipation prevents the excitation of random Gaussian patterns, as well as other modes such as the whispering gallery modes. Moreover, increasing the boundary dissipation, e.g. by lowering the fluid level, should eventually suppress all of the scars except the horizontal one (No. 2 in Table I). This is precisely what is observed in the experiment⁷.

Turning to the interaction effects, we first note that matrix elements off diagonal in scars, $I_{p,p'}^{(j)}$, are usually much smaller than the diagonal ones, $I_{p,p}^{(j)}$. The reason is that scars are localized objects, whereas the interaction between any two of them is proportional to their intersection area.

Consider, therefore, the scattering from a scar to itself. Here, the wave vectors, k and k' , are either parallel or antiparallel, except for small regions of self intersections. Thus the diagonal matrix elements of a scar associated with an orbit, p , which has a time reversal counterpart $-p$ (such as Nos. 3–9 in Table I) are $I_{p,p}^{(1)} \simeq I_k^{(1)}(0)$, $I_{p,-p}^{(1)} \simeq I_k^{(1)}(\pi)$ and $I_{p,p}^{(2)} \simeq I_k^{(2)}(0)$. The interaction matrix elements of scars associated with self retracing orbits (such as No. 1, 2, and 10 in Table I) are $I_{p,p}^{(1)} = I_{p,p}^{(2)} \simeq (I_k^{(1)}(0) + I_k^{(1)}(\pi) + I_k^{(2)}(0))/2$.

If only one scar is excited, its amplitude can be evaluated exactly from the steady state limit of Eq. (3). For scars associated with self retracing orbits, the result is

$$n_p^{(1)} = \frac{1}{2T} \sqrt{h^2 - h_p^2}, \quad (18)$$

where $T = \text{Re } I_{p,p}^{(1)}$. We assumed that the system was at resonance, $\omega = \text{Re } \omega_p$, and neglected the imaginary part of $I_{p,p}^{(j)}$.

Let now two scars be in resonance with the driving frequency, one can calculate the amplitude of the scar p in the presence of the second scar p' by perturbation theory in the off diagonal matrix element between these scars. The result is

$$n_p^{(2)} \simeq n_p^{(1)} (1 - \tau_1 Q - \tau_2 Q^2) \quad (19)$$

where $\tau_j = \text{Re } I_{pp'}^{(j)}/2T$ and $Q = n_{p'}^{(1)}/n_p^{(1)}$. According to Eq. (19) even a relatively weak interaction can suppress the scar with the higher threshold amplitude. Thus one should expect to observe only the dominating scar.

Finally, we comment on the role of discrete symmetries in the shape of the container. The exact eigenfunctions in this case can be classified according to the irreducible representation of the corresponding symmetry group. In

the case of the stadium billiard this symmetry is not sufficient to produce an exact degeneracy of eigenvalues. However, the eigenfrequencies of scars, associated with an excitation of a set of modes, are degenerate. The scars associated with orbits Nos. 3, 4 and 11 in Table I can be used as examples. The symmetry between the scars is usually weakly broken by perturbations such as inhomogeneous pumping or deviation from an exact horizontal state of the container. Interaction, in turn, drives the system into a nonsymmetric wave pattern.

To summarize, we have shown that Faraday wave patterns in a container of non-integrable boundary shape are mainly scars. The instability threshold for these patterns is determined by bulk dissipation, Lyapunov exponents, and dissipation near the container side walls. The latter is too strong for random patterns and whispering gallery modes to appear. Nonsymmetric wave patterns, in a symmetric container, take place due to the existence of degenerate scars and interaction effects between them.

We are grateful to Arshad Kudrolli and Jerry Gollub for many discussions and communications, and for the experimental data presented in this Letter. This research was supported by Grant No. 9800065 from the USA-Israel Binational Science Foundation (BSF).

-
- ¹ E. J. Heller, Phys. Rev. Lett. **53**, 1515 (1984); Lecture Notes in Physics **263**, 162 (1986).
 - ² J. Stein and H. -J. Stöckman, Phys. Rev. Lett. **68**, 2867 (1992); S. Sridhar and E. J. Heller, Phys. Rev. A **46**, 1728 (1992); A. Kudrolli, V. Kidambi, and S. Sridhar, Phys. Rev. Lett. **75**, 822 (1995).
 - ³ T. M. Fromhold, L. Eaves, F. W. Sheard, T. J. Foster, M. L. Leadbeater, and P. C. Main, Physica B **201**, 367 (1994); Phys. Rev. Lett. **72**, 2608 (1994).
 - ⁴ R. Blumel I. H. Davidson, W. P. Reinhardt, H. Lin, M. Sharnoff, Phys. Rev. A **45**, 2641 (1992).
 - ⁵ E. B. Bogomolny, Physica **D31**, 169 (1988); M. V. Berry, Proc R. Soc. Lond. **A423**, 219 (1989); O. Agam and S. Fishman, Phys. Rev. Lett. **73**, 806 (1994).
 - ⁶ M. C. Cross and P. C. Hohenberg, Rev. Mod. Phys. **65**, 851 (1993).
 - ⁷ A. Kudrolli, M. C. Abraham and J. P. Gollub, nlin.CD/0002045 (2000).
 - ⁸ T. B. Benjamin and J. C. Scott, J. Fluid Mech. **92**, 241 (1979).
 - ⁹ V. S. L'vov *Wave Turbulence Under Parametric Excitation* (Springer-Verlag, Berlin 1994).
 - ¹⁰ S. T. Milner, J. Fluid Mech. **225**, 81 (1991).
 - ¹¹ V. E. Zakharov, V. S. L'vov and S. S. Starobinets, Sov. Phys.-Usp **17**, 896 (1975).
 - ¹² In the experiment of Kudrolli et al.⁷, $\omega_c \approx 2\pi \cdot 100 \text{ sec}^{-1}$, and the explored frequency range is 55-70 Hz.
 - ¹³ T. B. Benjamin and F. Ursell, Proc. R. Soc. Lond. **A225**, 505 (1954).
 - ¹⁴ C. C. Mei, and L. F. Liu, J. Fluid Mech. **59**, 239 (1973); L. M. Hocking J. Fluid Mech. **179**, 253 (1987).